35th Annual International Conference of the IEEE EMBS
Osaka, Japan, 3 - 7 July, 2013

Motion Artifact Suppression in the ECG Signal by Successive Modifications in Frequency and Time

Suba R. Subramaniam, *Student Member, IEEE*, *EMBS,* Bingo Wing-Kuen Ling, and Apostolos Georgakis, *Member, IEEE*

***Abstract*— Ambulatory electrocardiogram signals can be contaminated with various types of noise. Among these, electrode motion 'em' artifacts are considered particularly undesired as they can be mistaken for ectopic beats. Unfortunately, 'em' noise has proved difficult to tackle using ordinary filtering techniques. In this paper, we explore a novel filtering alternative, and show that it could be considered as a potential candidate for dealing with electrode motion artifacts. The proposed system is composed of two simple parts: a frequency filter and a time window, interconnected in series. The two components are designed such that the overall system operates optimally in the mean square error sense. Experimentation on signals obtained from the MIT-BIH database demonstrates the superiority of the above approach over optimal Fourier filtering.**

I. INTRODUCTION

Electrocardiogram (ECG) signals are measurements of the bioelectrical activity of the heart and are widely used for the diagnosis of cardiovascular diseases. A particularly useful type of ECG is the one acquired during graded exercise assessment – stress testing – of the subject on a cardiovascular machine. Stress ECG is more likely to reveal certain underlying heart conditions in contrast to ECG recordings from a resting patient. On the other hand, the acquisition of ECG during the subject's activity is a difficult task resulting in a signal corrupted with various types of interference. Electrode motion artifact [1] – annotated as 'em' by clinicians on ECG recordings – is generally considered to be particularly unwanted among those interferences since it can pass as ectopic beats [4]. It is therefore crucial to remove this distortion prior to any clinical evaluation of the ECG.

Filtering electrode motion artifact out of the ECG is a non-trivial task because this interference overlaps with the useful signal in both the time and the frequency domains [1]. Consequently, any basic pass-band type filter would not be able to suppress noise components and preserve useful signal information at the same time. This situation calls for some alternative denoising approach. Indeed, there has been ongoing research on this topic (e.g. see [2], [3] and references therein). Most proposed methods have shown encouraging results, and come with their relative advantages and limitations; however, it can be argued that they all represent early-stage works.

In this paper, we contribute to the above research effort by proposing a simple filtering system of two cascaded components; a filter operating in frequency and a window applied in time. To understand the rationale, and appreciate the potential benefits of such a scheme one can consider the following example. Assume two distinct signal elements submerged in noise as depicted in Fig.1. It can be observed that a significant amount of noise still resides within the horizontal strip defined by a Fourier filter's cut-off thresholds. On the contrary, the combined effect of the frequency filter cascaded with a time window is that this signal is better isolated. Clearly, the overall system faces a higher signal-to-noise (SNR) ratio inside its pass band and is therefore in a more favorable position to suppress the overlapping interference.

We investigate the above idea with the aim of producing an effective motion artifact suppression method for the ECG. In order to design the proposed two-stage filtering system we first formulate a mean square error (MSE) minimization problem, and we then derive its solution. Since the statistics of the motion interference are not known, provision has been made so that such knowledge is not a prerequisite to the design of the system. Experimentation with the proposed method was based on ECG data obtained from the MIT-BIH noise stress test database [4], [5]. Finally, to demonstrate the superiority of the cascaded system we carried out comparisons with an optimized Fourier filter, using the same set of data.

II. DESIGN OF THE PROPOSED SYSTEM

A. System Configuration

The motivation behind this work is that by modifying the signal consecutively in the frequency and the time domains it may be possible to create a system that can better suppress interference as compared to a Fourier filter on its own. Drawing upon the simple example of Fig. 1 we may assume that the above is feasible, at least for signals with similar time-frequency characteristics. By examining the pseudo Wigner distribution of a noiseless ECG recording (Fig. 2a) it becomes apparent that this signal does consist of distinct higher-frequency elements (corresponding to QRS complexes) (Fig. 2b). Fig. 2c shows the same ECG segment corrupted by motion artifact noise of 6dB SNR.

Manuscript received January 21, 2013.
S. R. Subramaniam (e-mail: suba.r.subramaniam@kcl.ac.uk) is with the Division of Engineering, King's College London, WC2R 2LS, UK.
A. Georgakis (tel: 00442078481101; fax: 00442078482932; e-mail: apostolos.georgakis@kcl.ac.uk) is with the Division of Engineering, King's College London, WC2R 2LS, UK.
Bingo Wing-Kuen Ling (e-mail: yongquanling@gdut.edu.cn) is with the Faculty of Information Engineering, Guangdong University of Technology, Guangzhou 51006, China.

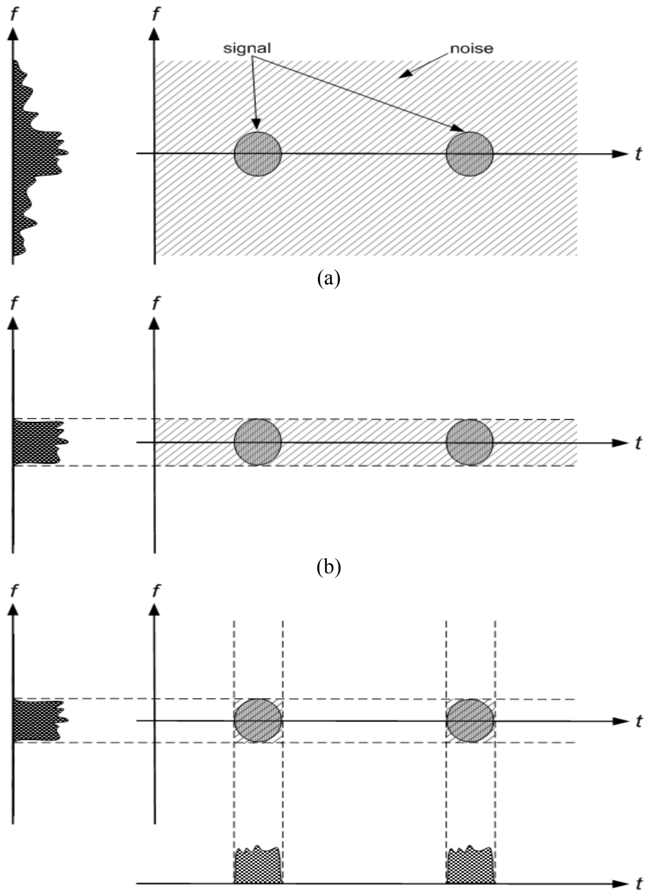

Figure 1. Joint time-frequency visualization of: (a) an assumed signal with two distinct elements embedded in noise; (b) a low-pass filtered version of the signal, and (c) the signal after its successive modifications by a frequency filter and a time window.

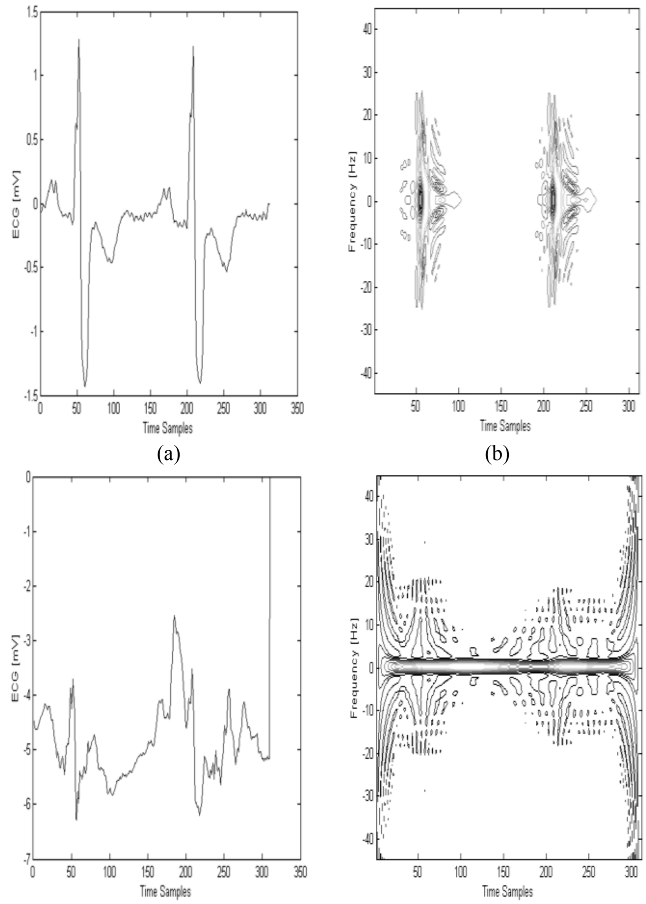

Figure 2. (a) A segment of a clean ECG signal, (b) the corresponding time-frequency plot, (c) the above segment corrupted with 'em' noise at 6dB SNR, (d) time-frequency plot of the noisy ECG.

It is evident that the useful waveform is now severely distorted, and that its frequency content is obscured across time (Fig. 2d).

The configuration of the proposed system is shown in Fig. 3. The signal is first passed through a linear time-invariant filter. The result is then multiplied with an appropriate time window. Since the input to the time window depends on the output of the filter, the two components cannot be designed independently. In the next paragraphs we describe how their joint optimization is implemented.

B. *Optimization of the Cascaded System Components*

For the purpose of this work, we denote our discrete signals as column vectors of size N. The goal of the filter is to find an estimate $\hat{\boldsymbol{x}}$ which would be as close as possible to the ideal $\boldsymbol{x}$. A natural optimality criterion is the mean square error (MSE),

$$\mathrm{mse}(\hat{\boldsymbol{x}}) = \frac{1}{\mathrm{N}} \mathrm{E}[\|\hat{\boldsymbol{x}} - \boldsymbol{x}\|^2] \,, \tag{1}$$

where $\|\boldsymbol{z}\|^2$ denotes the 2-norm of the vector $\boldsymbol{z}$, that is, $\|\boldsymbol{z}\|^2 = \boldsymbol{z}^H \boldsymbol{z}$. Equation (1) can be approximated by taking the average error over M realisations of the data,

$$\frac{1}{M} \sum_{i=1}^{M} \|\hat{\boldsymbol{x}}_i - \boldsymbol{x}_i\|^2, \tag{2}$$

where $\boldsymbol{x}_i$ is the i^{th} realisation of $\boldsymbol{x}$. Further, based on the filter circuit of Fig. 3, the estimate $\hat{\boldsymbol{x}}$ can be obtained as:

$$\hat{\boldsymbol{x}} = W F_{-1} G F \boldsymbol{y} \,, \tag{3}$$

where $\boldsymbol{y}$ represents the noisy observations; $F_{\,(\mathrm{NxN})}$ and $F_{-1(\mathrm{NxN})}$ are the discrete Fourier transform (DFT) matrices which correspond to the Fourier transform and inverse Fourier transform, respectively; $G_{(\mathrm{NxN})}$ and $W_{(\mathrm{NxN})}$ are diagonal matrices whose elements are composed of the filter's frequency response $\boldsymbol{g}$ and time window samples $\boldsymbol{w}$, respectively. That is, $\boldsymbol{g} = diag(G) = (g_0, \dots, g_{N-1})$ and $\boldsymbol{w} = diag(W) = (w_0, \dots, w_{N-1})$. The objective is then to determine the vector pair $\boldsymbol{g_{opt}}$ and $\boldsymbol{w_{opt}}$ that minimises (2). We are considering both $\boldsymbol{g_{opt}}$ and $\boldsymbol{w_{opt}}$ to be real-valued.

By substituting (3) into (2) we obtain the following cost function:

$$J(\boldsymbol{g}, \boldsymbol{w}) = \frac{1}{M} \sum_{i=1}^{M} \|W F_{-1} G F \boldsymbol{y}_i - \boldsymbol{x}_i\|^2 \tag{4}$$

Let,

$$\boldsymbol{a}_i = [a_{i,0} \dots \dots \; a_{i,N-1}]^T = F \boldsymbol{y}_i \,,$$

so that (4) becomes

$$J(\boldsymbol{g}, \boldsymbol{w}) = \frac{1}{M} \sum_{i=1}^{M} \|W F_{-1} G \boldsymbol{a}_i - \boldsymbol{x}_i\|^2$$
$$= \frac{1}{M} \sum_{i=1}^{M} (W F_{-1} G \boldsymbol{a}_i - \boldsymbol{x}_i)^H \, (W F_{-1} G \boldsymbol{a}_i - \boldsymbol{x}_i) \tag{5}$$

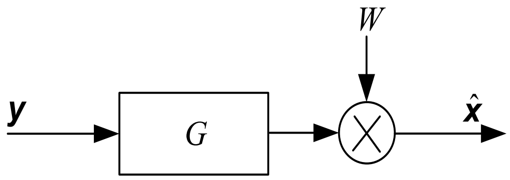

Figure 3. Proposed system configuration.

It can be observed that since G is a diagonal matrix then,

$$G\boldsymbol{a}_i = A_i\boldsymbol{g} \ ,$$

where $A_{i(\mathrm{NxN})}$ is a diagonal matrix such that $\boldsymbol{a}_i = diag(A_i)$. Now (5) can be further simplified as:

$$J(\boldsymbol{g},\boldsymbol{w}) = \frac{1}{M}\sum_{i=1}^{M}(W\bar{A}_\iota\boldsymbol{g} - \boldsymbol{x}_i)^H (W\bar{A}_\iota\boldsymbol{g} - \boldsymbol{x}_i) \quad (6)$$

where $\bar{A}_{\iota(\mathrm{NxN})}$ is equal to $F_{-1}A_i$. Expanding (6) yields:

$$J(\boldsymbol{g},\boldsymbol{w}) = \frac{1}{M}\sum_{i=1}^{M}(\boldsymbol{g}^H\bar{A}_\iota^{\ H}W^HW\bar{A}_\iota\boldsymbol{g} - \boldsymbol{g}^H\bar{A}_\iota^{\ H}W^H\boldsymbol{x}_i - \boldsymbol{x}_i^{\ H}W\bar{A}_\iota\boldsymbol{g} + \boldsymbol{x}_i^{\ H}\boldsymbol{x}_i)$$

$$= \frac{1}{M}\sum_{i=1}^{M}\left(\boldsymbol{g}^H\bar{A}_\iota^{\ H}W^HW\bar{A}_\iota\boldsymbol{g} - 2Re(\boldsymbol{x}_i^{\ H}W\bar{A}_\iota\boldsymbol{g}) + \boldsymbol{x}_i^{\ H}\boldsymbol{x}_i\right),$$

since $\boldsymbol{g}$ and $\boldsymbol{w}$ are real-valued, the above equation becomes:

$$\frac{1}{M}\sum_{i=1}^{M}\left(\boldsymbol{g}^TQ_{w,i}\boldsymbol{g} + \boldsymbol{b}_{w,i}^{\ T}\boldsymbol{g} + c_i\right) \quad (7)$$

where the matrix $Q_{w,i\ (\mathrm{NxN})}$, the column vector $\boldsymbol{b}_{w,i}$, and the scalar c_i are:

$$Q_{w,i} = \bar{A}_\iota^{\ H}W^HW\bar{A}_\iota = \bar{A}_\iota^{\ H}WW\bar{A}_\iota \ ,$$
$$\boldsymbol{b}_{w,i} = (-2Re(\boldsymbol{x}_i^{\ H}W\bar{A}_\iota))^T \ ,$$
$$c_i = \boldsymbol{x}_i^{\ H}\boldsymbol{x}_i = \|\boldsymbol{x}_i\|^2 \ .$$

Finally, (7) can be expressed as:

$$J(\boldsymbol{g},\boldsymbol{w}) = \boldsymbol{g}^TQ_w\boldsymbol{g} + \boldsymbol{b}_w^{\ T}\boldsymbol{g} + c \ , \quad (8)$$

with $Q_w = \frac{1}{M}\sum_{i=1}^{M}Q_{w,i}$, $\boldsymbol{b}_w = \frac{1}{M}\sum_{i=1}^{M}\boldsymbol{b}_{w,i}$, and $c = \frac{1}{M}\sum_{i=1}^{M}c_i$

We seek the vector $\boldsymbol{g_o}$ that minimizes (8), thus, the following equation must be solved:

$$\left.\frac{\partial J(\boldsymbol{g},\boldsymbol{w})}{\partial \boldsymbol{g}}\right|_{\boldsymbol{g}=\boldsymbol{g_o}} = 0 \ . \quad (9)$$

The derivative of the first term of (8) with respect to the vector $\boldsymbol{g}$ is in general equal to:

$$\frac{\partial\{\boldsymbol{g}^TQ_w\boldsymbol{g}\}}{\partial \boldsymbol{g}} = Q_w\boldsymbol{g} + Q_w^{\ T}\boldsymbol{g} \quad , \quad (10)$$

Likewise, for the second term we have,

$$\frac{\partial\{\boldsymbol{b}_w^{\ T}\boldsymbol{g}\}}{\partial \boldsymbol{g}} = \boldsymbol{b}_w \ . \quad (11)$$

Based on (10) and (11), (9) can be re-written as

$$\left(Q_w + Q_w^{\ T}\right)\boldsymbol{g_o} + \boldsymbol{b}_w = 0 \ . \quad (12)$$

The system of N linear equations in N unknowns defined in (12) can then be solved to specify the designed filter's frequency response $\boldsymbol{g_o}$.

In a similar manner we next solve for $\boldsymbol{w_o}$. From (6), it can be observed that since W is a diagonal matrix then,

$$W\bar{A}_\iota\boldsymbol{g_o} = \tilde{Z}_\iota\boldsymbol{w}$$

where $\tilde{Z}_{\iota(\mathrm{NxN})}$ is a diagonal matrix so that $\bar{A}_\iota\boldsymbol{g_o} = diag(\tilde{Z}_\iota)$. Now (6) can be re-written as:

$$J(\boldsymbol{g},\boldsymbol{w}) = \frac{1}{M}\sum_{i=1}^{M}\left(\tilde{Z}_\iota\boldsymbol{w} - \boldsymbol{x}_i\right)^H\left(\tilde{Z}_\iota\boldsymbol{w} - \boldsymbol{x}_i\right) \quad (13)$$

Expanding (13) leads to:

$$\frac{1}{M}\sum_{i=1}^{M}\left(\boldsymbol{w}^TQ_{g,i}\boldsymbol{w} + \boldsymbol{b}_{g,i}^{\ T}\boldsymbol{w} + c_i\right) \quad (14)$$

Where the matrix $Q_{g,i\ (\mathrm{NxN})}$, the column vector $\boldsymbol{b}_{g,i}$, and the scalar c_i are:

$$Q_{g,i} = \tilde{Z}_\iota^{\ H}\tilde{Z}_\iota \ ,$$
$$\boldsymbol{b}_{g,i} = (-2Re(\boldsymbol{x}_i^{\ H}\tilde{Z}_\iota))^T \ ,$$
$$c_i = \boldsymbol{x}_i^{\ H}\boldsymbol{x}_i = \|\boldsymbol{x}_i\|^2 \ .$$

Then, (14) can be expressed as:

$$J(\boldsymbol{g},\boldsymbol{w}) = \boldsymbol{w}^TQ_g\boldsymbol{w} + \boldsymbol{b}_g^{\ T}\boldsymbol{w} + c \ , \quad (15)$$

with $Q_g = \frac{1}{M}\sum_{i=1}^{M}Q_{g,i}$, $\boldsymbol{b}_g = \frac{1}{M}\sum_{i=1}^{M}\boldsymbol{b}_{g,i}$, and $c = \frac{1}{M}\sum_{i=1}^{M}c_i$.

The vector $\boldsymbol{w_o}$ that minimizes (15) can be obtained as the solution of the following linear system:

$$\left(Q_g + Q_g^{\ T}\right)\boldsymbol{w_o} + \boldsymbol{b}_g = 0 \ . \quad (16)$$

Since both (12) and (16) require knowledge of $\boldsymbol{w_o}$ and $\boldsymbol{g_o}$ respectively, an iterative procedure is adopted as follows:

Step 1: Initialize W and G to identity matrices and set $k = 0$.
Step 2: Solve for $\boldsymbol{g_{o,k}}$ using (12)
Step 3: Based on the $\boldsymbol{g_{o,k}}$, obtain $\boldsymbol{w_{o,k}}$ using (16)
Step 4: Iterate Steps 2 and 3 until the solution converges.

III. EXPERIMENTATION

The ECG data used in this study were obtained from the MIT-BIH noise stress test database [4], [5]. The database contains two clean ECG records along with their corresponding distorted versions. The electrode motion - noise used in the distorted versions was acquired from the limbs of physically active volunteers during typical ambulatory recordings; it can thus be viewed as realistic motion noise. For each clean ECG record six different noisy versions are available, containing 'em' noise at six different SNR levels.

We have segmented both the clean and the distorted ECG data into two-cycle epochs, and have used $M = 10$ randomly chosen epoch pairs in order to optimize the filtering system. The resulting system was then applied to previously unseen epochs.

To demonstrate the validity of the original assumption, i.e. that the proposed two-stage system can outperform a single filter in enhancing the ECG, we have processed the same set of data with an optimized Fourier filter. This was designed using the derivations of Section II.B by simply setting W equal to an identity matrix, and solving the resulting set of linear equations (12). The same set of the ten epoch pairs used for the optimization of the two-stage system was also employed for determining the optimal single filter.

To quantify the performance of the two compared approaches, the root-mean-square error (RMSE) and the normalized correlation coefficient (NCC) [6] were used. The NCC was calculated as,

$$NCC = \frac{\sum_{n=1}^{N} x(n)\hat{x}(n)}{\sqrt{\sum_{n=1}^{N} x^2(n) \sum_{n=1}^{N} \hat{x}^2(n)}} \quad , \qquad (17)$$

where N is the signal length, $x(n)$ is the desired signal and $\hat{x}(n)$ is the filtered signal. The results of the experiments are listed in Table 1, where it is clear that the proposed method consistently outperforms the single-stage filter at all noise levels both in terms of the RMSE and the NCC measures. Figs. 4 and 5 show an example segment of a filtered ECG signal based on the above approaches for two different noise levels.

IV. CONCLUSIONS

We have investigated a filtering scheme for possible application to the removal of motion artifacts from stress ECG signals. The method is based on a two-stage system comprising a linear time-invariant filter and a time window. The overall system was designed based on the MSE minimization criterion, and the two components were optimized accordingly. The presented method only depends on the availability of few cycles of clean ECG. Knowledge of the noise statistics (e.g. the autocorrelation function of the noise) is not required in the computations for the optimal system, which is an advantage over Wiener-type solutions. Preliminary experimentation has indicated encouraging performance. Future work will have to focus on thorough experimentation, and address questions regarding the development of the proposed concept into a clinical real-world system.

REFERENCES

[1] N.V. Thakor and Y. Zhu, "Applications of adaptive filtering to ECG analysis: Noise Cancellation and Arrhythmia Detection," IEEE Trans. Biomed. Eng., Vol. 38, No. 8, pp. 785-794, 1991.

[2] M. Kirst, B. Glauner, and J. Ottenbacher, “Using DWT for ECG Motion Artifact Reduction with Noise-correlating Signals,” 2011 Annual International Conference of the IEEE Engineering in Medicine and Biology Society (EMBC), pp. 4804-4807, 2011.

[3] P. Mithun, P. C. Pandey, T. Sebastian, P. Mishra, and V. K. Pandey,“A Wavelet Based Technique for Suppression of EMG Noise and Motion Artifact in Ambulatory ECG,” 2011 Annual International Conference of the IEEE Engineering in Medicine and Biology Society (EMBC), pp. 7087-7090, 2011.

[4] G. B. Moody, W. K. Muldrow, and R. G. Mark, "A noise stress test for arrhythmia detectors," Computers in Cardiology, pp. 381-384384: IEEE Comput. Soc. Press, 1984.

[5] G.B. Moody, R.G. Mark, and A. L. Goldberger, “PhysioNet: a Web-based resource for the study of physiologic signals”, IEEE Eng. Med. and Biol. Mag., vol. 20, no. 3, pp. 70-75, 2001.

[6] Y. F. Wu and R. M. Rangayyan, “An algorithm for evaluating the performance of adaptive filters for the removal of artifacts in ECG signals,” in Proc. 20th Canadian Conf. Elec. and Comp. Engineering, pp. 864-867, 2007.

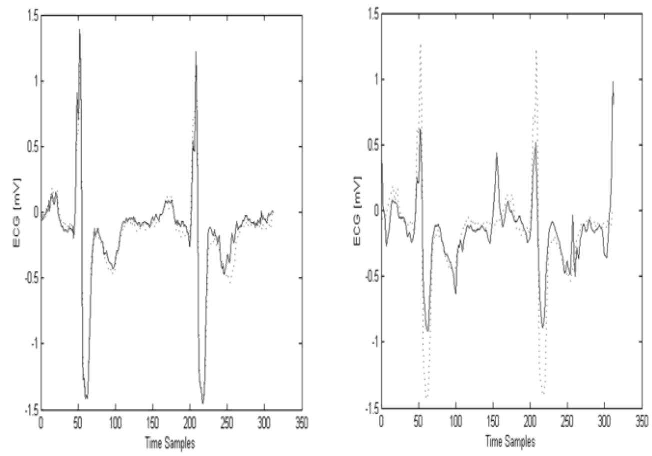

(a) (b)

Figure 4. Filtered ECG signal after applying: (a) the proposed method (solid line), and (b) a single optimized Fourier filter (solid line). The ideal ECG is also shown (dotted lines). The contaminated ECG contained electrode motion noise of 18dB SNR.

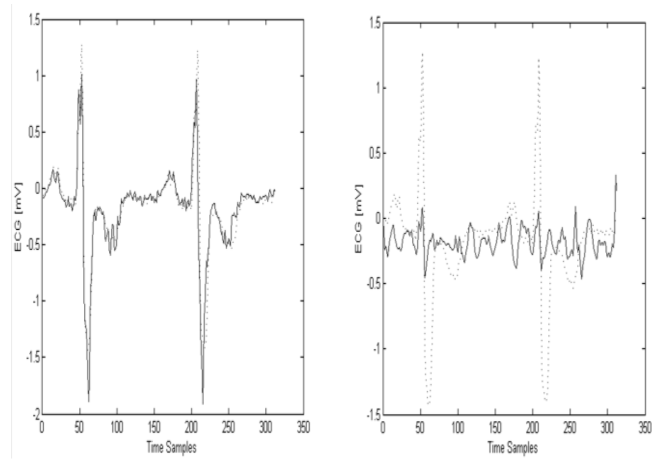

(a) (b)

Figure 5. Filtered ECG signal after applying: (a) the proposed method (solid line), and (b) a single optimized Fourier filter (solid line). The ideal ECG is also shown (dotted lines). The contaminated ECG contained electrode motion noise of 0dB SNR.

TABLE 1

RMSE AND NCC VALUES OF THE FILTERED ECG SIGNALS CORRESPONDING TO DIFFERENT LEVELS OF ELECTRODE MOTION ARTIFACT DENOISED WITH THE PRESENTED METHOD AND A SINGLE OPTIMIZED FOURIER FILTER

Method \ SNR(dB)		24	18	12	6	0	-6
Proposed	RMSE	0.0595	0.0721	0.1003	0.2005	0.1532	0.1391
	NCC	0.9905	0.9859	0.9724	0.9007	0.9354	0.9531
Optimized Fourier Filter	RMSE	0.2110	0.2239	0.2568	0.3144	0.3670	0.3910
	NCC	0.8811	0.8653	0.8165	0.6918	0.5207	0.4152